Insight into the Structural Role of Carotenoids in the Photosystem I: A Quantum Chemical Analysis

Yanli Wang, Lisong Mao, and Xiche Hu
Department of Chemistry, University of Toledo, Toledo, Ohio

ABSTRACT The structural stabilization role of carotenoids in the formation of photosynthetic pigment-protein complexes is investigated theoretically. The π–π stacking and CH-π interactions between β-carotenes and their surrounding chlorophylls (and/or aromatic residues) in Photosystem I (PS1) from the cyanobacterium *Synechococcus elongatus* were studied by means of the supermolecular approach at the level of the second-order Møller-Plesset perturbation method. PS1 features a core integral antenna system consisting of 22 β-carotenes intertwined with 90 chlorophyll molecules. The binding environments of all 22 β-carotenes were systematically analyzed. For 21 out of the 22 cases, one or more chlorophyll molecules exist within van der Waals' contacts of the β-carotene molecule. The calculated strengths of π–π stacking interactions between the conjugated core of β-carotene and the aromatic tetrapyrrole rings of chlorophyll are substantial, ranging from -3.54 kcal/mol for the perpendicular-positioned BCR4004···CHL1217 pair to -16.01 kcal/mol for the parallel-oriented BCR4007···CHL1122 pair. A strong dependence of the π–π stacking interaction energies on the intermolecular configurations of the two interacting π-planes is observed. The parallel-oriented β-carotene and chlorophyll pair is energetically much more stable than the perpendicular-positioned pair. The larger the extent of π–π overlapping, the stronger the interaction strength. In many cases, the β-ring ends of β-carotene molecules are found to interact with the tetrapyrrole rings of chlorophyll via CH-π interactions. For the latter interactions, the calculated interaction strengths vary from -7.03 to -11.03 kcal/mol, depending on the intermolecular configuration. This work leads to the conclusion that π–π stacking and CH-π interactions between β-carotene and their surrounding chlorophylls and aromatic residues play an essential role in binding β-carotenes in PS1 from *S. elongatus*. Consequently, the molecular basis of the structural stabilization function of carotenoids in formation of the photosynthetic pigment-protein complexes is established.

INTRODUCTION

Photosynthesis is a biological reaction of great importance, not only because it provides the basis for all life on earth but also because it represents an efficient model system for conversion of solar energy into chemical energy. Photosynthetic organisms have developed complex and efficient apparatus to harvest the light of the Sun and to convert the light energy into chemical energy (Hu et al., 2002). The photosynthetic membranes of these organisms contain thousands of pigment molecules, mainly chlorophylls and carotenoids. The latter are noncovalently bound to proteins to form well-organized pigment-protein complexes (Zuber and Cogdell, 1995; Hu et al., 2002). In the last two decades, crystal structures of many pigment-protein complexes have largely become known. Structures of the photosynthetic reaction center for *Rhodopseudomonas viridis* (Deisenhofer et al., 1985) as well as for *Rhodobacter spheroides* (Allen et al., 1987; Ermler et al., 1994) were determined to atomic resolution by x-ray crystallography. High resolution crystal structures of the light-harvesting complex-II (LH-II) from two species (*Rps. acidophila* and *Rhodospirillum molischianum*) have been resolved (McDermott et al., 1995; Koepke et al., 1996). Most recently, a 2.5 Å resolution crystal structure of Photosystem I (PS1) from *Synechococcus elongatus* has been reported (Jordan et al., 2001). These crystal structures provide detailed knowledge of the organization of pigment molecules in the photosynthetic membrane necessary for understanding structure and function of the photosynthetic apparatus. We are interested in the structural stabilization role of carotenoids in formation of the pigment-protein complexes.

Carotenoids play multiple roles in photosynthesis, including light harvesting, photoprotection, and structural stabilization (Fraser et al., 2001; Cogdell and Frank, 1987; Moskalenko and Karapetyan, 1996). The light-harvesting and photoprotection functions of carotenoids are well understood (Fraser et al., 2001; Cogdell and Frank, 1987; Ritz et al., 2000; Hsu et al., 2001; Hu et al., 2002). As accessory light-harvesting pigments, carotenoids absorb energy in a spectral region complementary to that of chlorophylls, and transfer energy to the major pigments (i.e., chlorophylls). Most importantly, as photoprotective agents, carotenoids quench the excited triplet state of chlorophylls. The latter state would otherwise be long-lived and could readily react with molecular oxygen to generate singlet oxygen, which causes the photooxidative destruction of membranes (Cogdell and Frank, 1987; Nilsson et al., 1972). In contrast, the structural stabilization role of carotenoids is less well characterized. A wealth of data has been accumulated which indicated that carotenoids are necessary for the assembly and stabilization of certain pigment-protein complexes in the photosynthetic bacteria

Submitted August 18, 2003, and accepted for publication December 9, 2003.

Address reprint requests to Asst. Prof. Xiche Hu, University of Toledo, Dept. of Chemistry, 2801 W. Bancroft St., Toledo, OH 43606. Tel.: 419-530-1513; E-mail: xhu@utoledo.edu.

0006-3495/04/05/3097/15 $2.00

and in plants (Moskalenko and Karapetyan, 1996; Zurdo et al., 1993; Lang and Hunter, 1994; Lokstein et al., 2002). But the detailed mechanism for such a structural stabilization role of carotenoids is not clear. Based on careful examination of all known crystal structures of photosynthetic pigment-protein complexes (Deisenhofer et al., 1985; Allen et al., 1987; McDermott et al., 1995; Koepke et al., 1996; Jordan et al., 2001; Hofmann et al., 1996), we discovered that all carotenoids are surrounded either by aromatic residues or by chlorophylls (Wang and Hu, 2002b). We hypothesize that the π–π stacking and CH-π interactions are the molecular forces that bind carotenoids in the pigment-protein complexes. In Wang and Hu (2002b), we calculated the strengths of π–π stacking interactions between a carotenoid and its surrounding aromatic residues in the LH-II complex of *Rs. molischianum* by high level ab initio electronic structure calculations. The second order Møller-Plesset perturbation method (MP2) calculations yielded a total stabilization energy of -15.66 kcal/mol between the carotenoid molecule lycopene and its four surrounding aromatic residues. Even in the case of water-soluble peridine-chlorophyll-protein complex of *Amphidinium carterae*, the π–π stacking interactions between the carotenoid molecule peridinins and their surrounding aromatic groups (aromatic residues and chlorophyll-a) were found to play a role in binding peridinins (Mao et al., 2003). In this article, we extend the quantum chemical analysis of intermolecular interactions into PS1 from cyanobacterium *S. elongatus*. As detailed below, in addition to π–π stacking interactions, CH-π interactions are also operative in PS1.

The photosynthetic membranes of oxygenic photosynthetic organisms employ a Z-scheme consisting of two photosynthetic systems, i.e., Photosystem I (PS1) and Photosystem II (PS2) (Golbeck, 1992; Barber, 2003). Structural details of PS1 from *S. elongatus* has been reported by Jordan et al. (2001). In contrast to the bacterial photosynthetic reaction center, which collects light energy through separate membrane-intrinsic light-harvesting complexes, PS1 from *S. elongatus* features a core integral antenna system consisting of 90 chlorophyll molecules and 22 carotenoids. The specific forms of all carotenoids in PS1 were identified as β-carotene (Jordan et al., 2001). How are the pigments bonded to proteins to form a sophisticated pigment-protein complex like PS1? To address this question, one needs to understand the intermolecular forces that govern pigment-protein and pigment-pigment interactions. According to our working hypothesis, the π–π stacking interactions and CH-π interactions between β-carotene and its surrounding aromatic residues and chlorophylls are the dominant molecular forces that bind β-carotenes in PS1. The strength of these intermolecular interactions in PS1 from *S. elongatus* is characterized by means of high level ab initio electronic structure calculations. As detailed below, the 22 carotenoid molecules are surrounded by a variety of aromatic groups, i.e., chlorophylls and aromatic residues, in close van der Waals contact. Such a multitude of intermolecular configurations provide us with a great opportunity to study dependence of π–π stacking interactions on the intermolecular configuration (orientation, distance, and extent of π–π overlapping) in a biologically important complex system.

The π–π stacking interactions play an important role in a large number of biological and chemical systems, including base-stacking in DNA, molecular recognition, aromatic crystal packing, and biomolecular self-aggregation. They have been the subject of great theoretical interest ever since the early days of London (Kim et al., 2000; Sponer et al., 2000; Chalasinski and Szczesniak, 2000; Eisenschitz and London, 1930; Hobza and Zahradnik, 1988; Chalasinski and Gutowski, 1988; Buckingham et al., 1988). One of the most widely studied systems is the benzene dimer, which serves as the prototype for aromatic π–π stacking (Karlstrom et al., 1983; Hobza et al., 1994, 1996; Tsuzuki et al., 1996, 2000; Jaffe and Smith, 1996). The intricate interplay of π–π stacking and hydrogen-bonding in DNA basepairing has been extensively studied by Hobza and co-workers (Sponer et al., 2000, 1996a).

Two valuable lessons were learned from these studies of weakly bonded complexes:

1. The π–π stacking interactions, as one form of weakly bonded interaction, are essentially a juxtaposition of several elements, including electrostatic interactions, exchange repulsion interactions, induction, and dispersion forces. Of these, dispersion forces constitute the dominant attractive forces between neutral molecules (Hobza and Zahradnik, 1988; Chalasinski and Gutowski, 1988; Buckingham et al., 1988). Dispersion forces arise from the mutual correlation of electrons that belong to interacting monomers (intermolecular correlation effects); the correlation energy is typically of the same order of magnitude as the intermolecular interaction energy. Consequently, inclusion of electron correlation is important in any accurate ab initio electronic structure calculation of weakly bonded complexes (Sponer et al., 1996a, 2000; Kim et al., 2000; Del Bene and Shavitt, 1997).
2. For a proper treatment of correlation energy in the interacting dimer, inclusion of diffuse basis sets is required (Sponer et al., 1996a; Tsuzuki et al., 1996).

There are three principal methods that include the correlation correction:

1. Configuration interaction (CI) methods.
2. Coupled cluster (CC) methods.
3. Many-body perturbation theory, also known as Møller-Plesset perturbation theory (MP).

The full CI expansion is only of theoretical value due to its prohibitive computational intensity. Other variants of CI methods do not satisfy the necessary requirement of size

consistency for treating intermolecular complexes. Coupled cluster methods—in particular, the coupled cluster method with single, double, and perturbative triple excitations, CCSD(T)—have been successfully applied to weakly bonded complexes of small molecules (Hobza and Sponer, 1996; Tsuzuki et al., 1998, 2000, 2002; Hobza et al., 1996). The largest intermolecular complexes studied at the CCSD(T) level so far are the benzene dimer (Hobza et al., 1996; Tsuzuki et al., 2002) and the naphthalene dimer (Tsuzuki et al., 2000). However, CCSD(T) is very demanding in computational resources in terms of the CPU speed, size of the core memory, and capacity of the hard disk. It is impractical to apply the CCSD(T) method to large biomolecular systems. A popular and feasible way to include the correlation effects is the second-order Møller-Plesset perturbation theory (MP2), which usually covers a significantly large part of the correlation energy. The MP2 method has been applied to a wide variety of weakly bonded complexes, including π–π stacking and hydrogen-bonding in DNA, van der Waals complexes of atoms and molecules, etc. (Sponer et al., 2000, 1996a; Kim et al., 2000; Del Bene and Shavitt, 1997). One of the largest aromatic dimer systems studied at the MP2 level of theory to date is the MP2/6-31G* calculation of bacteriochlorophyll dimer in the photosynthetic reaction center of the purple bacterium *Rb. spheroides* (Wang and Hu, 2002a).

It should also be pointed out that the density functional theory (DFT) approach is gaining popularity for treating large biomolecules due to its low computing cost for including the correlation effect. Unfortunately, the DFT method is found inadequate for treating weakly bonded intermolecular complexes dominated by dispersion interactions due to absence of long-range correlations in density functionals (Sponer et al., 1996a; Tsuzuki and Luthi, 2001). Many schemes have been developed to correct this deficiency of DFT method by incorporating an extra damped dispersion interaction term (Elstner et al., 2001; Wu et al., 2001; Wu and Yang, 2002). Applicability of such schemes to treating weakly bonded intermolecular interactions remains a subject of hot debate (van Mourik and Gdanitz, 2002).

In this article, we implement the second-order Møller-Plesset perturbation method to calculate the strength of intermolecular interactions between carotenoids and their surrounding aromatic groups (i.e., chlorophylls and aromatic residues) in PS1 from the cyanobacterium *S. elongatus*. Our primary objective is to study the contribution of π–π stacking and CH-π interactions and their dependence on the intermolecular configuration. The rest of the article is organized as follows. In Binding Environment of β-Carotenes in PS1, below, we review structural details of pigment organization in PS1 from *S. elongatus*, with special emphasis on the surroundings of carotenoids. Detailed implementation of the MP2 method, along with the choice of basis set, is described in Methods. Following that, Results and Discussion presents intermolecular interaction strengths and their configuration dependence, as well as an analysis of the physical origin of intermolecular forces. A brief summary is given in Conclusions.

BINDING ENVIRONMENT OF β-CAROTENES IN PS1

The cyanobacterial PS1 exists as a trimer in vivo. The 2.5 Å resolution crystal structure of PS1 reveals that each monomer contains nine transmembrane subunits (PsaA, PsaB, PsaF, PsaI, PsaJ, PsaK, PsaL, PsaM, and PsaX) in α-helical conformation and three stromal subunits (PsaC, PsaD, and PsaE) coordinating 127 cofactors. Among the latter are 96 chlorophyll-a molecules and 22 carotenoids, mainly β-carotenes in this case. The molecular structures of β-carotene and chlorophyll-a are depicted in Fig. 1. The 22 carotenoids are in van der Waals contact ($<$3.6 Å) to 60 chlorophyll-a molecules, which facilitates energy transfer from carotenoids to chlorophylls for the light-harvesting functions and the quenching of chlorophyll triplet state for the photoprotection function. The interaction between carotenoid and chlorophyll in close geometric proximity has been widely studied in the context of the light-harvesting and photoprotection role (de Weerd et al., 2003; Naqvi, 1980; Gillbro et al., 1988; Hu et al., 1997). Here, our interest is in the third role of carotenoid and chlorophyll stacking, i.e., the structure-stabilization role.

The binding environments of β-carotenes were systematically analyzed; chlorophylls and aromatic residues within 5.0 Å of the β-carotene molecule were identified and displayed with the program VMD (Humphrey et al., 1996). It was found that each of the 22 β-carotene molecules is surrounded by chlorophylls and/or aromatic residues. Table 1 lists all the chlorophylls and aromatic residues that are in close contact with each β-carotene molecule. For 21 out of the 22 cases, there exists at least one chlorophyll molecule within van der Waals contacts of the β-carotene molecule; and in some cases, the β-carotene molecule is surrounded by more than one chlorophyll. As shown in Fig. 1, β-carotene is a conjugated linear molecule with a β-ring attached at both ends. Due to its lack of polar or charged groups, the β-carotene molecule cannot form either a normal hydrogen-bond or saltbridge with its surrounding residues in protein. However, a strong π–π stacking interaction can arise as β-carotene comes into close contact with aromatic residues and/or chlorophyll-a molecules that contain highly conjugated tetrapyrrole rings. Another potential force for binding β-carotene is CH-π interaction (Nishio et al., 1995). Depending on intermolecular configurations, there are three ways for β-carotene to form intermolecular interactions with chlorophyll: 1), the conjugated core of β-carotene approaches the tetrapyrrole planes of chlorophyll (BCR-core$\cdots$CHL-core π–π stacking interactions); 2), the β-ring end of β-carotene meets the tetrapyrrole planes of chlorophyll (BCR-head$\cdots$CHL-core CH-π interactions); and 3),

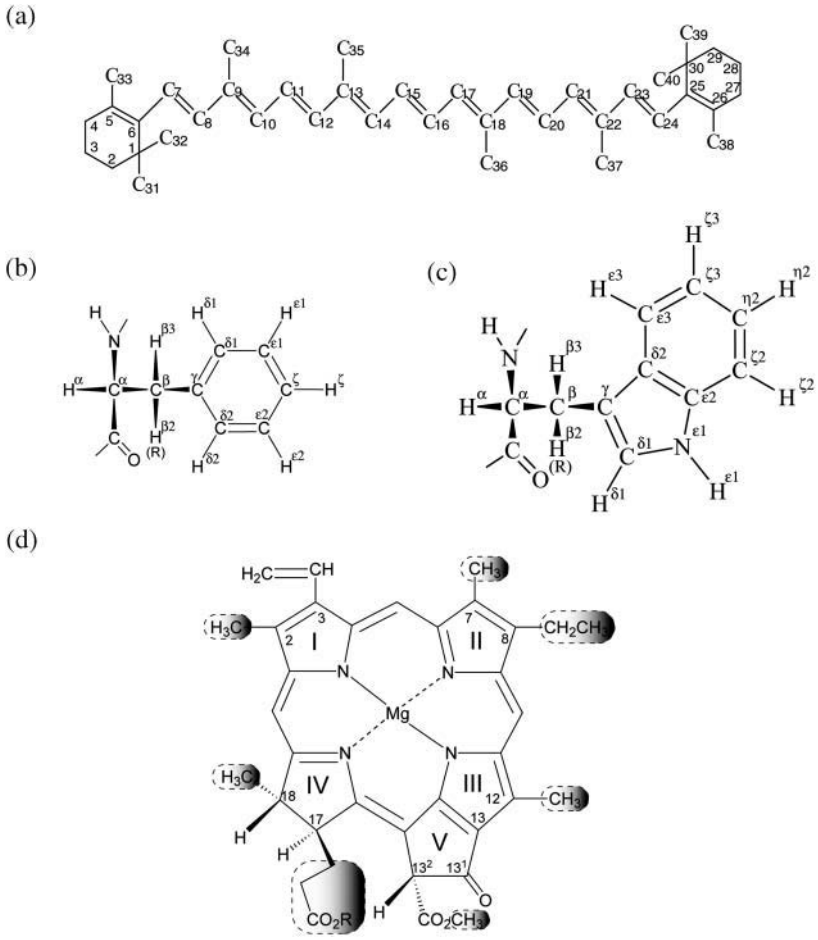

FIGURE 1 Molecular structures of intermolecular interaction partners. (*a*) β-carotene with all hydrogen atoms omitted; (*b*) phenylalanine; (*c*) tryptophan; and (*d*) chlorophyll-a. Carbon atoms are labeled in accord with the IUPAC-IUB carbon numbering system (IUPAC-IUB, 1986). The nonpolar side groups indicated by the shaded squares in chlorophyll-a indicate groups that are replaced by H-atoms in the MP2/6-31G*(0.25) calculations.

the hydrophobic phytol tail of chlorophyll encounters the conjugated core of β-carotene (BCR-core$\cdots$CHL-tail CH-π interactions). The hydrophobic binding environment of one of the β-carotene molecules, BCR4017, is representative. As shown in Fig. 2, BCR4017 is involved in π–π stacking interactions with one chlorophyll (CHL1239) and in CH-π interactions with another chlorophyll (CHL1206). Phytol tails of several chlorophylls (CHL1022, CHL1131, and CHL1239) are in van der Waals contact with the conjugated core of BCR4017, forming BCR-core$\cdots$CHL-tail CH-π interactions. In addition, three aromatic residues (PsaA-F45, PsaB-W654, and PsaB-F658), one methionine (PsaB-M655), and one asparagine (PsaA-N445) are also in geometric proximity of BCR4017. Hereafter, the focus of this study will mainly be on BCR-core$\cdots$CHL-core π–π stacking interactions and BCR-head$\cdots$CHL-core CH-π interactions. Due to the limit of scope, the analysis of BCR-core$\cdots$CHL-tail CH-π interactions will be briefly presented, and for comparison purposes only.

Listed in Table 1 is a group classification for each of the 22 β-carotenes. On the basis of a systematic examination of the binding pockets of all 22 β-carotenes, β-carotenes were classified into six different groups according to position and orientation of their surrounding chlorophylls:

In *group A*, β-carotene is surrounded by three chlorophylls (one chlorophyll has extended π–π stacking contact in the middle of β-carotene, whereas the other two chlorophylls contact two ends of β-carotene).

In *group B*, β-carotene is in contact with two chlorophylls (one chlorophyll with extended π–π-stacking contact in the middle of β-carotene, whereas the other meets the end of β-carotene).

In *group C*, β-carotene is sandwiched between two chlorophylls.

In *group D*, the end-ring of β-carotene meets only one chlorophyll.

In *group E*, β-carotene is in extended π–π stacking contact with two chlorophylls in the middle of the β-carotene molecule, and meets another chlorophyll at the end of β-carotene ring.

In *group F*, β-carotene is in extended π–π stacking contact with only one chlorophyll in the middle of β-carotene.

METHODS

The intermolecular interaction energy was calculated at the MP2/6-31G*(0.25) level with frozen-core by means of the supermolecular

TABLE 1 Carotenoids (β-carotenes) and their surrounding aromatic groups in Photosystem I of *S. elongatus*

Groups*	β-carotene†	Chlorophylls within 5 Å†	Aromatic residues within 5 Å†
Group A	BCR4001	CHL1113, CHL1118, CHL1120	—
	BCR4004	CHL1212, CHL1217, CHL1218	PsaB-F224
	BCR4015	CHL1229, CHL1235, CHL1303	PsaB-F431
	BCR4018	CHL1132, CHL1204, CHL1207	—
Group B	BCR4008	CHL1124, CHL1133	—
	BCR4010	CHL1222, CHL1231	PsaB-F390
	BCR4013	CHL1101, CHL1302	PsaA-W118
	BCR4016	CHL1228, CHL1701	—
	BCR4017	CHL1206, CHL1239	—
	BCR4019	CHL1201, CHL1502	PsaI-F31
Group C	BCR4014	CHL1229, CHL1301	—
Group D	BCR4003	CHL1127	—
	BCR4005	CHL1225	—
	BCR4011	CHL1126	PsaA-F681, PsaA-W744
	BCR4012	CHL1230	—
	BCR4021	CHL1201	—
Group E	BCR4020	CHL1131, CHL1207, CHL1502	PsaI-W20
Group F	BCR4002	CHL1112	—
	BCR4006	CHL1211	—
	BCR4007	CHL1122	PsaA-F415
	BCR4009	CHL1220	PsaB-F318

There exists a total of 22 carotenoids., i.e., β-carotenes (BCR), in PS1 of *S. elongatus* (Jordan et al., 2001). Chlorophylls (Chls) and aromatic residues within 5 Å of carotenoids are listed here.

*β-carotenes were classified into six different groups according to their binding environment (see text).

†The naming convention for polypeptide chains, chlorophylls, and carotenoids follows Jordan et al. (2001), and the residue identification numbers are in accord with the PDB file for the PS1 (accession No. 1JB0). The prefixes PsaA-, PsaB-, PsaI-, and PsaL- indicate various subunits of PS1.

approach. In the supermolecular approach, the electronic Schrödinger equations for the dimer AB, and the two monomers A and B,

$$\hat{H}_i\psi(i) = E_i\psi(i) \quad i = AB, A, B, \tag{1}$$

are solved. Here, $\hat{H}_i$, $\psi(i)$, and E_i are the Hamiltonian, wave function, and energy for the molecular species **i**, respectively. The energy of interaction between molecules A and B is defined as the difference between the energy of the interacting dimer E_{AB} and the energies of the monomers E_A and E_B,

$$\Delta E = E_{AB} - E_A - E_B. \tag{2}$$

In our calculations, the coordinates of nonhydrogen atoms in β-carotenes and their interacting partners (i.e., chlorophylls and aromatic residues; see Fig. 3) were extracted from the 2.5 Å x-ray crystal structure of PS1 from *S. elongatus* (Jordan et al., 2001; PDB accession number 1JB0). Therefore, the internal coordinates of the monomers used in computing E_A and E_B are the same as within the dimer AB.

As in all other quantum mechanical calculations, the quality of calculated results depends on the choice of the basis set. As mentioned earlier, for a proper treatment of π–π stacking interactions, inclusion of diffuse basis sets is required (Sponer et al., 1996a; Tsuzuki et al., 1996). These diffuse basis sets are localized sufficiently far from the atomic nuclei, and thus fill the empty space between two interacting monomers. The latter is where a substantial portion of correlation energy originates. At the MP2 level, Dunning's correlation consistent basis sets (cc-pVXZ, X=D, T, Q, and 5) and the augmented aug-cc-PVXZ basis sets are desirable, and have been applied to both π–π stacking and hydrogen-bonding complexes of small molecules (Tsuzuki et al., 1998; Tarakeshwar et al., 2001). However, such huge basis sets are not computationally feasible for the large system of our interest here. A more feasible choice for our system is a medium sized basis set, such as the polarization augmented double ζ 6-31G* basis set. In a series of studies of DNA base-stacking, Hobza and co-workers employed a modified 6-31G* basis set with diffuse (momentum-optimized, dispersion-energy-optimized) d-polarization at the MP2 level of theory (Sponer et al., 2000, 1996a,b; Kratochvil et al., 2000). In the conventional 6-31G* basis set, the d-polarization functions for nonhydrogen atoms (C, N, and O atoms) are energy-optimized with an exponent of 0.8. In the modified basis set, an exponent of 0.25 is used for the d-polarization functions of C, N, and O atoms, instead. Following the author's convention (Sponer et al., 2000; Hobza et al., 1995), the modified basis set is designated 6-31G*(0.25). Inclusion of more diffused d-polarization functions in the 6-31G*(0.25) basis set improves the electron correlation stabilization energy of stacked

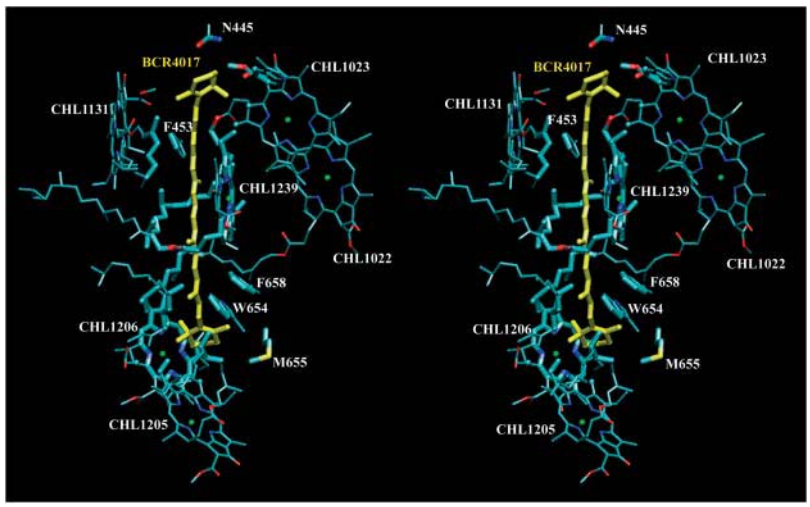

FIGURE 2 Stereo pairs of the binding pocket of the β-carotene molecule BCR4017 based on the 2.5 Å resolution crystal structure of PS1 from *S. elongatus* (Jordan et al., 2001). All atoms within 5 Å of BCR4017 are represented in a thick licorice representation whereas atoms beyond 5 Å are thinner. The entire BCR4017 molecule is in yellow; other atoms are color-coded with oxygen atom in red, nitrogen atom in blue, carbon atom in cyan, and sulfur atom in yellow. (Produced with the program VMD; Humphrey et al., 1996.)

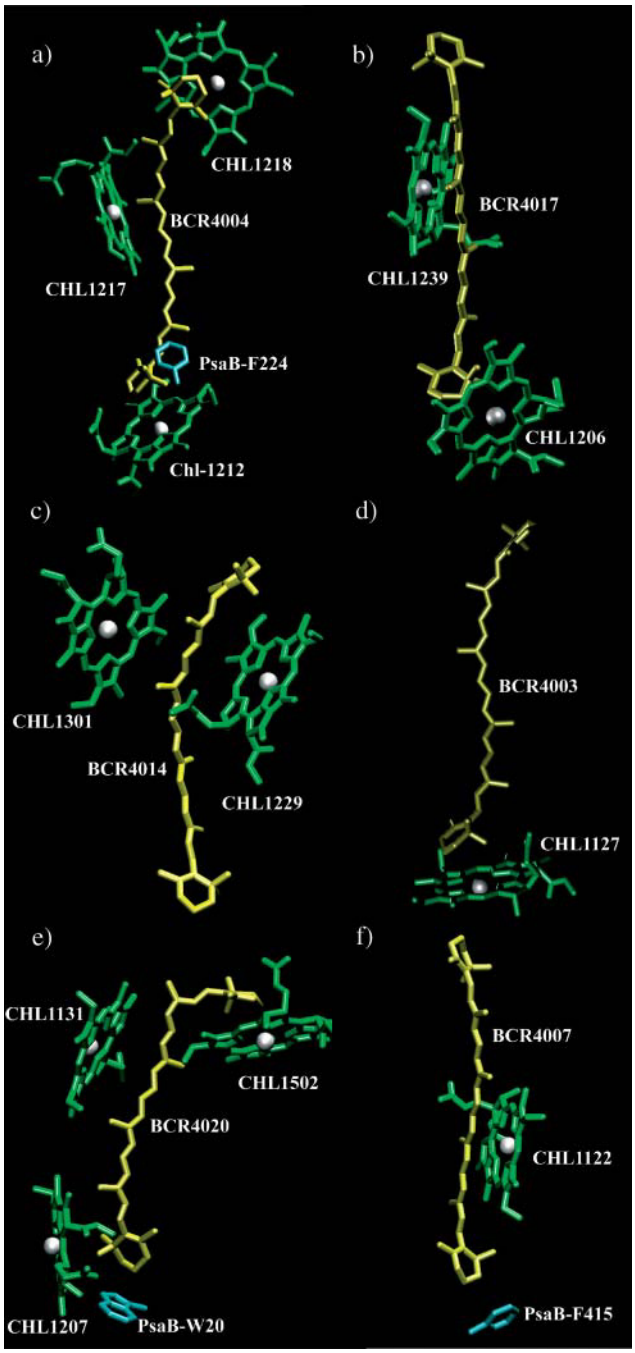

FIGURE 3 Representative aromatic surroundings of carotenoids in PS1 of the cyanobacterium *S. elongatus* (Jordan et al., 2001). The PS1 contains a total of 22 carotenoids that can be grouped into six classes according to their surrounding chlorophylls. Only representatives for each of the six groups are shown here. The labeling for each panel coincides with the group classification as listed in Table 1. The phytol tails of chlorophylls are truncated for clarity.

DNA base dimers substantially (Sponer et al., 2000; Hobza et al., 1997). A recent comparison of MP2/6-31G*(0.25) treatment of DNA base-stacking with that of the theoretical more rigorous CCSD(T) has shown that MP2/6-31G*(0.25) recovered 75–90% of the intermolecular correlation stabilization energy (Hobza and Sponer, 2002). The 6-31G*(0.25) basis set was adopted in all of our calculations.

All the calculations were carried out using the GAUSSIAN98 program (Frisch et al., 1998) on a LINUX workstation cluster in our laboratory and on a Itanium 2 cluster at the Ohio Supercomputer Center. The basis set superposition error (BSSE) is corrected by the Boys and Bernardi Counter Poise method (Boys and Bernardi, 1970).

In addition to the intermolecular interaction energy, we are also interested in determining the physical origin of intermolecular interactions. In particular, we want to find out contributions of electrostatic interaction and dispersion force to the overall interaction strength for a particular intermolecular interaction. In the variational supermolecular approach adopted here, the correlation component of the MP2 interaction energy corresponds primarily to the dispersion interaction energy, as well as correlation corrections to the electrostatic interaction and induction force. The upper bound of dispersion interaction energy can be estimated as the correlation energy; the latter is simply the difference between the MP2 energy and the Hartree Fock (HF) energy. The electrostatic interaction energies were analyzed by means of the distributed multipole method of Stone and co-workers as implemented in the program ORIENT 3.2 (Stone et al., 1995). Distributed multipoles (Stone, 1985) themselves are evaluated from the GAUSSIAN98 output wavefunctions by means of the GDMA 1.0 program (Stone et al., 1995).

RESULTS AND DISCUSSION

The strengths of π–π stacking and CH-π interactions, as well as their dependence on intermolecular configurations (distance, angle, and extent of π–π overlapping) are studied. Because of the high demand on CPU time and system memory for implementing the MP2 calculations of the current system, it is impractical to treat all intermolecular interactions involving all 22 carotenoids. Instead, we only chose one representative β-carotene from each of the six groups listed in Table 1. Fig. 3 depicts all six representatives for the six groups of β-carotenes. The labeling for each panel in Fig. 3 coincides with the group classification of Table 1. In Fig. 3 *A*, the β-carotene molecule BCR4004 is in contact with one phenylalanine side chain (PsaB-F224) and three chlorophylls, of which two chlorophylls (CHL1212 and CHL1218) meet the β-carotene molecule at both ends and the remaining (CHL1217) in the middle. The conjugated π-system of BCR4004 is nearly perpendicular to the tetrapyrrole rings of CHL1217. The methyl groups of the β-ring point to the aromatic ring of PsaB-F224, forming CH-π interactions. In Fig. 3 *B*, two chlorophylls are interacting with the β-carotene molecule BCR4017. One of the chlorophylls (CHL1239) is parallel to the π-plane of BCR4017. The other one (CHL1206) interacts with the β-ring of BCR4017. In Fig. 3 *C*, the β-carotene molecule BCR4014 is sandwiched between two chlorophyll molecules, CHL1229 and CHL1301. The tetrapyrrole plane of CHL1301 is nearly parallel to the π-plane of BCR4014 and that of CHL1229 is almost perpendicular. In Fig. 3 *D*, there is only one chlorophyll CHL1127 in close contact with the β-carotene molecule BCR4003. The chlorophyll CHL1127 meets the β-carotene molecule at its β-ring end. In Fig. 3 *E*, the β-carotene molecule BCR4020 is in van der Waals contact with three chlorophylls (CHL1131, CHL1207, and CHL1502) and one tryptophan side chain (PsaB-W20). The

chlorophyll molecule CHL1502 is interacting with both the β-ring end and the long conjugated chain of the β-carotene BCR4020. CHL1131 interacts extensively with the π-plane of BCR4020 while CHL1207 approaches the β-ring end of BCR4020. The crossing angle between the π-planes of chlorophylls and β-carotene is 59.6° for CHL1131. The indole ring of the tryptophan residue PsaB-W20 is nearly perpendicular to the β-ring of BCR4020, forming CH-π interactions. In Fig. 3 *F*, the β-carotene molecule BCR4007 only interacts with one chlorophyll (CHL1122) and one side chain of a phenylalanine residue (PsaB-F415). The tetrapyrrole plane of CHL1122 is parallel to the π-plane of BCR4007 with a crossing angle of 177.7°. The phenyl ring of PsaB-F415 and the head of BCR4007 are involved in CH-π interactions.

The MP2/6-31G*(0.25) calculations of the intermolecular interaction strengths between β-carotene and their surrounding aromatic groups were carried out in a pairwise manner. For CH-π interactions between β-carotene and aromatic residues, the entire β-carotene molecule and the side-chain atoms of aromatic residues are included in the MP2/6-31G*(0.25) calculation; the α-carbon atom and its associated main-chain groups are excluded (see Fig. 1). The α-carbon itself is replaced by a hydrogen atom. The β-carotene···Trp and β-carotene···Phe pairs contain a total of 115 and 111 atoms, respectively. With the 6-31G*(0.25) basis set, the β-carotene···Trp complex consists of 366 electrons with a total of 880 basis functions (1660 primitive Gaussians); the β-carotene···Phe complex contains 346 electrons with a total of 833 basis functions (1572 primitive Gaussians).

For π–π stacking and CH-π interactions between β-carotene and the chlorophyll-a molecule, the combined total of 233 atoms (137 atoms in chlorophyll-a and 96 atoms in β-carotene) far exceeds the memory and disk capacity of currently available computers. To proceed, both the chlorophyll-a and the β-carotene molecules are truncated. For the chlorophyll-a molecule, the phytol tail is omitted, and other nonpolar side groups are replaced by hydrogen atoms as depicted in Fig. 1. The replaced nonpolar side groups are indicated in shaded squares in Fig. 1, including the methyl groups associated with C-2, C-7, C-12, and C-18, the ethyl group on C-8, and the entire 17-propionic-acid side chain. The guiding principle for replacement of groups and atoms on chlorophyll-a and β-carotene is to retain the essential tetrapyrrole plane of chlorophyll-a and the conjugated π-system of β-carotene. For the β-carotene molecules, the truncation is dependent upon the region of the molecule that is geometrically close to the π-system of chlorophyll. Listed in Table 2 are deleted atoms and groups in each interacting pair. The number for each carbon atom in β-carotene is adopted from the PDB file, and is labeled as shown in Fig. 1. In general, for the methyl groups that are directly bonded to the conjugated π-system of β-carotene (i.e., C33, C34, C35, C36, C37, and C38), the group is retained if it is close to the β-carotene···chlorophyll interaction site; otherwise, it is replaced with a H-atom. For the two β-rings at both ends of the β-carotene molecule, the entire ring is kept if it is in close contact with the interacting chlorophyll; if the β-ring is far from the interacting site, the single-bond carbon atoms on the ring (C1, C2, C3, C4 or C27, C28, C29, and C30) and the two methyl groups (C31 and C32 or C39 and C40) are deleted. Fig. 4 depicts the structures of interacting carotenoid···chlorophyll pairs after truncation of nonessential carbon atoms.

TABLE 2 The carbon atoms omitted in calculations

Intermolecular pair	Label	Atoms on β-carotene deleted*
BCR4004···CHL1212	p-1	27,28,29,30,34,35,36,37,38,39,40
BCR4004···CHL1217	p-2	31,32,33,34,35,37,38,39,40
BCR4004···CHL1218	p-3	1,2,3,4,31,32,33,34,35,36,37
BCR4004···PsaB–F224	No cutting	
BCR4017···CHL1239	p-4	1,2,3,4,27,28,29,30,31,32,33,34, 37,38,39,40
BCR4017···CHL1206	p-5	27,28,29,30,34,35,36,37,38,39,40
BCR4014···CHL1229	p-6	27,28,29,30,31,32,33,34,35,36, 37,38,39,40
BCR4014···CHL1301	p-7	27,28,29,30,31,32,33,36,37, 38,39,40
BCR4003···CHL1127	p-8	1,2,3,4,31,32,33,34,35,36,37
BCR4020···CHL1207	p-9	27,28,29,30,35,36,37,38,39,40
BCR4020···CHL1131	p-10	1,2,3,4,27,28,29,30,31,32,33,34, 38,39,40
BCR4020···CHL1502	p-11	1,2,3,4,31,32,33,34,35,37
BCR4020···PsaB–W20	No cutting	
BCR4007···CHL1122	p-12	1,2,3,4,27,28,29,30,31,32,33,37, 38,39,40
BCR4007···PsaB–F415	No cutting	

The numbers represent carbon atoms that are either deleted or replaced by hydrogen atoms on the β-carotene molecule to facilitate MP2/6-31G(0.25) calculations. The number for the carbon atoms in β-carotene is adopted from the PDB file 1JB0 as labeled in Fig. 1.

Table 3 lists the calculated HF/6-31G*(0.25) and MP2/6-31G*(0.25) energies for each molecular species involved in all the pairwise intermolecular interactions studied here. Based on these data, the intermolecular interaction energies for each interacting pair at both the MP2 and HF levels are calculated according to Eq. 2 and are listed in Table 4. The BSSE correction for each interaction is given in parentheses. Also listed in Table 4 are geometric data on intermolecular configuration for the interacting pair, including the crossing angle between two interacting π-planes, the closest atom-to-atom distance between the two interacting partners, and the center-to-center π–π displacement. The latter is only applicable to π–π stacking interactions, and measures the displacement of the center of one π-system against the other. Due to its conjugated long chain, the π-system of the β-carotene molecule is much longer than that of a chlorophyll molecule.

To adequately reflect the extent of overlapping of the π-plane of β-carotene with that of chlorophyll, the center-to-center π–π displacement is calculated by:

1. Locating the atom on the π-system of β-carotene with the closest distance to the central Mg atom of chlorophyll.

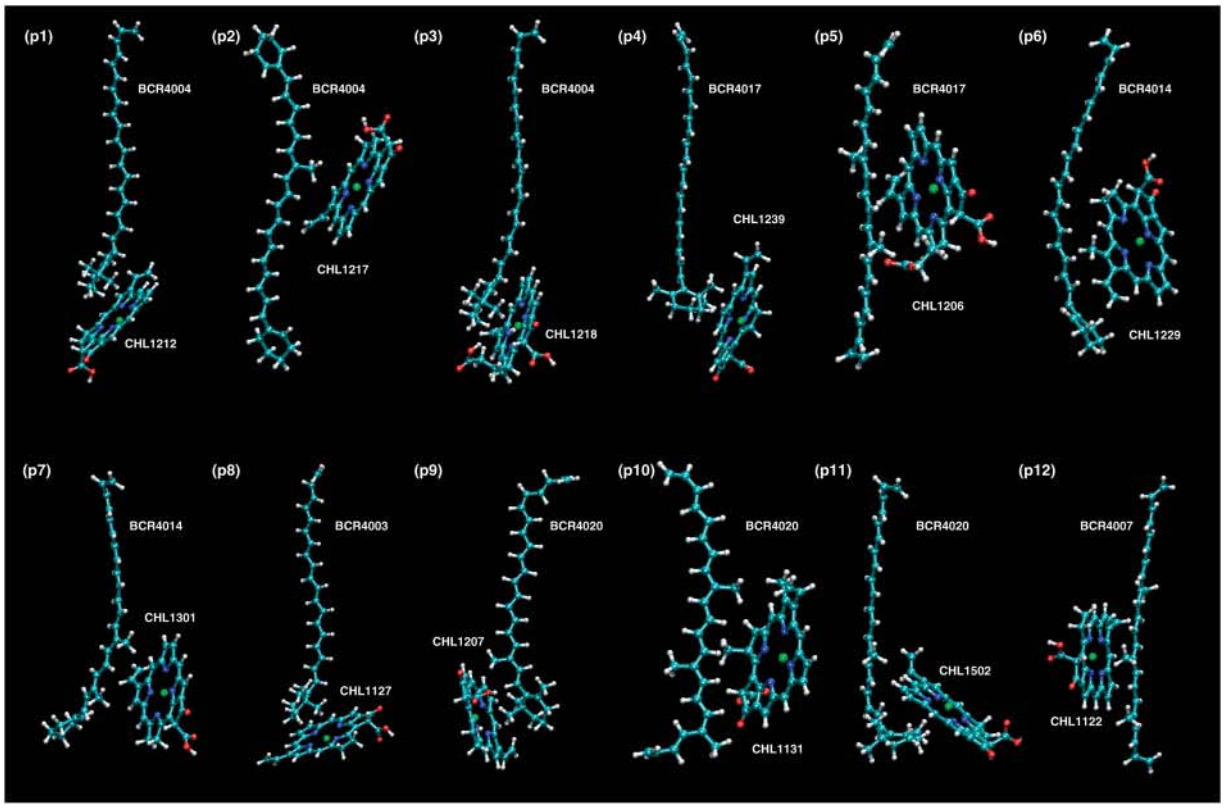

FIGURE 4 Structures of the interacting carotenoid···chlorophyll pairs after truncation of nonessential carbon atoms (see Table 2). The coordinates of nonhydrogen atoms are taken directly from the crystal structure (accession number 1JB0) (Jordan et al., 2001). The omitted carbon atom is replaced by a hydrogen atom as needed to satisfy valence. The positions of all hydrogen atoms are placed by ab initio geometry optimization at the HF/6-31G* level with all the nonhydrogen atom positions fixed. Labels for panels coincide with the corresponding labels in column 2 of Table 2.

2. Projecting the selected atom into the tetrapyrrole plane of chlorophyll and measuring its distance to the central Mg atom within the tetrapyrrole plane as the center-to-center π–π displacement.

Depending on the intermolecular configurations, the carotenoid-chlorophyll interactions analyzed in this study can be classified as either BCR-core···CHL-core π–π stacking interactions or BCR-head···CHL-core CH-π interactions. The former involves intermolecular contact between the conjugated π-plane of β-carotene with the tetrapyrrole plane of chlorophyll, and occurs in BCR4004···CHL1217, BCR4017···CHL1239, BCR4014···CHL1229, BCR4014···CHL1301, BCR4020···CHL1131, and BCR4007···CHL1122 pairs. The latter involves intermolecular contact between the β-ring end of β-carotene with the tetrapyrrole plane of chlorophyll, and shows up in BCR4004···CHL1212, BCR4004···CHL1218, BCR4017···CHL1206, BCR4003···CHL1127, and BCR4020···CHL1207 pairs. The intermolecular configurations of the BCR4020···CHL1502 pair belongs to both classes, containing a partial plane-plane contact in addition to the head-plane contact.

For the BCR-core···CHL-core π–π stacking interactions, the interaction between BCR4007···CHL1122 resulted in an attractive energy of −16.01 kcal/mol, which is the strongest. The weakest carotenoid-chlorophyll interaction energy of −3.54 kcal/mol is observed in the BCR4004···CHL1217 pair. As seen in Table 4, the conjugated π-plane of BCR4007 is nearly parallel to that of CHL1122, forming a plane-crossing angle of 177.7°. In contrast, the conjugated π-plane of BCR4004 is almost perpendicular to the tetrapyrrole plane of CHL1217 with a crossing angle of 99.0°. The arrangement with β-carotene approaching the π-plane of chlorophyll perpendicularly is known as *T-shaped edge-to-face configuration*. The much stronger π–π stacking interactions observed for the parallel configuration in the BCR4007···CHL1122 pair than for the T-shaped edge-to-face configuration in the BCR4004···CHL1217 pair are in sharp contrast to results of model studies on the benzene dimer (Hobza et al., 1996; Tsuzuki et al., 2002). π–π stacking interactions of the benzene dimer, as the prototype for aromatic π–π stacking, have been studied at various levels of ab initio theory, and the lowest energy structures of the dimer are found to be the T-shaped edge-to-face and parallel-displaced configurations (Hobza et al., 1996; Tsuzuki et al., 2002). The most recent CCSD(T) calculation suggests that the two configurations are nearly isoenergetic minima (Tsuzuki et al., 2002). It should be pointed out that in the model studies on

TABLE 3 MP2/6-31G*(0.25) and HF/6-31G*(0.25) energies for all molecular species of intermolecular pairs

Intermolecular pair	Molecular species	E_{HF} (Hartree)*	E_{MP2} (Hartree)*
BCR4004···CHL1212	BCR4004···CHL1212	−2716.359095	−2723.437173
	BCR4004···[GhostCHL1212]	−1118.643781	−1121.928053
	[GhostBCR4004]···CHL1212	−1597.724326	−1601.496325
	BCR4004	−1118.641741	−1121.923400
	CHL1212	−1597.720301	−1601.487637
BCR4004···CHL1217	BCR4004···CHL1217	−2793.272809	−2800.559621
	BCR4004···[GhostCHL1217]	−1195.541536	−1199.038804
	[GhostBCR4004]···CHL1217	−1597.739891	−1601.515169
	BCR4004	−1195.540365	−1199.035923
	CHL1217	−1597.737542	−1601.510258
BCR4004···CHL1218	BCR4004···CHL1218	−2981.952727	−2989.663542
	BCR4004···[GhostCHL1218]	−1118.642433	−1121.929295
	[GhostBCR4004]···CHL1218	−1863.323074	−1867.721297
	BCR4004	−1118.639559	−1121.922746
	CHL1218	−1863.317310	−1867.710542
BCR4004···PsaB–F224	BCR4004···PsaB − F224	−1816.413343	−1821.795273
	BCR4004···[GhostPsaB − F224]	−1546.747999	−1551.347206
	[GhostBCR4004]···PsaB − F224	−269.671581	−270.447353
	BCR4004	−1546.747374	−1551.345776
	PsaB−F224	−269.669863	−270.444479
BCR4017···CHL1239	BCR4017···CHL1239	−2787.917134	−2795.024377
	BCR4017···[GhostCHL1239]	−924.693661	−927.372670
	[GhostBCR4017]···CHL1239	−1863.236753	−1867.631758
	BCR4017	−924.688959	−927.364092
	CHL1239	−1863.230255	−1867.620310
BCR4017···CHL1206	BCR4017···CHL1206	−2716.364220	−2723.425834
	BCR4017···[GhostCHL1206]	−1118.643811	−1121.912823
	[GhostBCR4017]···CHL1206	−1597.726783	−1601.501802
	BCR4017	−1118.642263	−1121.909006
	CHL1206	−1597.723181	−1601.494101
BCR4014···CHL1129	BCR4014···CHL1129	−2638.309086	−2645.123713
	BCR4014···[GhostCHL1129]	−1001.566646	−1004.467812
	[GhostBCR4014]···CHL1129	−1636.753240	−1640.646621
	BCR4014	−1001.563627	−1004.462060
	CHL1129	−1636.750247	−1640.640675
BCR4014···CHL1301	BCR4014···CHL1301	−2677.353610	−2684.288098
	BCR4014···[GhostCHL1301]	−1079.622923	−1082.763673
	[GhostBCR4014]···CHL1301	−1597.734716	−1601.512291
	BCR4014	−1079.620664	−1082.759684
	CHL1301	−1597.731547	−1601.506698
BCR4003···CHL1127	BCR4003···CHL1127	−2716.362227	−2723.437229
	BCR4003···[GhostCHL1127]	−1118.634964	−1121.915922
	[GhostBCR4003]···CHL1127	−1597.735287	−1601.509388
	BCR4003	−1597.731166	−1601.501414
	CHL1127	−1118.633034	−1121.911553
BCR4020···CHL1207	BCR4020···CHL1207	−2755.383754	−2762.566238
	BCR4020···[GhostCHL1207]	−1157.659666	−1161.050623
	[GhostBCR4020]···CHL1207	−1597.729733	−1601.500546
	BCR4020	−1157.657665	−1161.045786
	CHL1207	−1597.723794	−1601.489334
BCR4020···CHL1131	BCR4020···CHL1131	−2639.488276	−2646.329470
	BCR4020···[GhostCHL1131]	−963.714170	−966.513468
	[GhostBCR4020]···CHL1131	−1675.784286	−1679.802454
	BCR4020	−963.711148	−966.506581
	CHL1131	−1675.778631	−1679.792399
BCR4020···CHL1502	BCR4020···CHL1502	−2755.377691	−2762.580725
	BCR4020···[GhostCHL1502]	−1157.664525	−1161.057294
	[GhostBCR4020]···CHL1502	−1597.723823	−1601.505854
	BCR4020	−1157.660512	−1161.049323
	CHL1502	−1597.718461	−1601.494613
BCR4020···PsaB–W20	BCR4020···PsaB − W20	−1947.144911	−1952.874281
	BCR4020···[GhostPsaB − W20]	−1546.748614	−1551.333995

(*Continued*)

TABLE 3 (*Continued*)

Intermolecular pair	Molecular species	E_{HF} (Hartree)*	E_{MP2} (Hartree)*
	[GhostBCR4020]···PsaB – W20	−400.404335	−401.536293
	BCR4020	−1546.747701	−1551.331315
	PsaB-W20	−400.401966	−401.530991
BCR4007···CHL1122	BCR4007···CHL1122	−2561.458887	−2568.078237
	BCR4007···[GhostCHL1122]	−963.732516	−966.542543
	[GhostBCR4007]···CHL1122	−1597.737286	−1601.510177
	BCR4007	−963.727371	−966.533060
	CHL1122	−1597.731020	−1601.498756
BCR4007···PsaB–F415	BCR4007···PsaB – F415	−1816.422490	−1821.800784
	BCR4007···[GhostPsaB – F415]	−1546.755005	−1551.348939
	[GhostBCR4007]···PsaB – F415	−269.670735	−270.448924
	BCR4007	−1546.754510	−1551.347604
	PsaB-F415	−269.669097	−270.446197

Energies at both the HF (E_{HF}) and the MP2 (E_{MP2}) levels are calculated using the modified 6-31G(0.25) basis set with diffuse d-polarization.

benzene dimer, optimized intermolecular configurations are utilized for calculating the intermolecular interaction energies, whereas the current calculations employ intermolecular configurations taken directly from the x-ray crystallographically determined structural coordinates. Another factor that potentially contributes to the much weaker interaction strength of the T-shaped edge-to-face BCR4004···CHL1217 pair is the smaller π–π overlapping. As seen in Table 4, the center-to-center π–π displacement is 3.18 Å and 0.34 Å for the BCR4004···CHL1217 pair and the BCR4007···CHL1122 pair, respectively.

The second strongest interaction strength of −12.52 kcal/mol for the BCR-core···CHL-core π–π stacking interactions occurs in the BCR4017···CHL1239 pair. The carotenoid molecule BCR4017 is also nearly parallel to CHL1239, forming a plane-crossing angle of 176.2°. However, the extent of π–π overlapping is significantly weaker in the BCR4017···CHL1239 pair than that in the BCR4007···CHL1122 pair, as indicated by the center-to-center π–π displacements listed in Table 4; BCR4017 only stacks with ring I of CHL1239 with a center-to-center π–π displacement of 2.58 Å, whereas BCR4007 and CHL1122 shows extended π–π stacking with a center-to-center π–π displacement of 0.34 Å . Furthermore, the closest atom-to-atom distance between BCR4017 and CHL1239 is 3.65 Å, which is slightly longer than that between BCR4007 and CHL1122 (3.53 Å).

In general, the strengths of π–π stacking interactions between β-carotenes and their surrounding aromatic groups display a strong configuration dependence on orientation (crossing angle), area of π–π overlapping, and distance between two interacting partners. As seen in Table 4, the

TABLE 4 MP2/6-31G*(0.25) and HF/6-31G*(0.25) pairwise intermolecular interaction energies and configuration dependence

Intermolecular pair	Angle* (degree)	Distance† (Å)	π–π Displacement‡ (Å)	ΔE_{HF}§ (kcal/mol)	ΔE_{MP2}§ (kcal/mol)
BCR-core···CHL-core π–π stacking interactions					
BCR4004···CHL1217	99.0	3.42	3.18	5.41 (2.21)	−3.54 (4.89)
BCR4017···CHL1239	176.2	3.65	2.58	8.33 (7.03)	−12.52 (12.57)
BCR4014···CHL1229	76.5	3.75	4.56	6.78 (3.77)	−5.82 (7.34)
BCR4014···CHL1301	167.8	3.66	4.39	2.53 (3.41)	−7.61 (6.01)
BCR4020···CHL1131	59.6	3.51	5.27	6.39 (5.44)	−8.50 (10.63)
BCR4007···CHL1122	177.7	3.53	0.34	6.85 (7.16)	−16.01 (13.12)
BCR-head···CHL-core CH-π interactions					
BCR4004···CHL1212	—	3.45	—	5.66 (3.81)	−8.03 (8.37)
BCR4004···CHL1218	—	3.62	—	8.02 (5.42)	−8.13 (10.86)
BCR4017···CHL1206	—	3.47	—	4.00 (3.23)	−7.03 (7.23)
BCR4003···CHL1127	—	3.41	—	5.03 (3.80)	−7.48 (7.75)
BCR4020···CHL1207	—	3.42	—	3.54 (4.98)	−9.46 (10.07)
BCR4020···CHL1502	—	3.58	—	6.69 (5.88)	−11.03 (12.06)
BCR···amino acid CH-π interactions					
BCR4004···PsaB–F224	—	3.24	—	3.91 (1.47)	−0.45 (2.70)
BCR4020···PsaB–W20	—	3.50	—	2.41 (2.06)	−2.51 (5.01)
BCR4007···PsaB–F415	—	3.50	—	2.04 (1.34)	−1.83 (2.55)

*Crossing angle between two interacting π-planes.

†Closest atom-to-atom distance between two interacting partners.

‡The π–π displacement measures the center-to-center displacement of two π-planes (see text); only shown for pairs with plane-plane conformation.

§Intermolecular interaction energies at both the HF (ΔE_{HF}) and the MP2 (ΔE_{MP2}) levels after BSSE correction. The BSSE value for each complex is shown in parentheses.

more extensive the overlapping area between the two interacting π-systems and the closer to 180° the plane-crossing angle, the stronger the π–π stacking interactions.

For BCR-head···CHL-core CH-π interactions, MP2/6-31G*(0.25) calculations result in CH-π interaction strengths between −7.03 kcal/mol and −11.03 kcal/mol for all five carotenoid–chlorophyll interactions (see above) with head-plane conformation. The following analysis established that the β-ring end of β-carotene is the main contributor to the interaction strength in the CH-π interactions. For one of the BCR-head···CHL-core pairs, BCR4017···CHL1206, MP2/6-31G*(0.25) calculations yield nearly identical interaction energy with or without the conjugated core of the β-carotene molecule BCR4017. When the conjugated core of BCR4017 is removed, the calculated intermolecular interaction strength is −6.72 kcal/mol, which is close to −7.03 kcal/mol for the complete pair. It is worth noting that these CH-π interaction energies represent a stabilization effect of significant magnitude. In contrast, such a head-plane conformation is not possible in the case of a headless linear conjugated carotenoid molecule lycopene which is the major form of carotenoid in LH-II from *Rs. molischianum* (Koepke et al., 1996; Wang and Hu, 2002b). It might be speculated that this stabilization effect by the β-ring ends of β-carotene could account for the widespread occurrence of the β-carotenes in nature.

The interactions between β-carotene and aromatic residues (phenylalanine or tryptophan) analyzed here are all of the CH-π interaction type. The strengths of these interactions range from −0.45 kcal/mol for the BCR4004···PsaB–F224 pair to −2.51 kcal/mol for the BCR4020···PsaB–W20 pair. For comparison, the intermolecular interactions between aromatic residues and the carotenoid molecule lycopene in the LH-II complex of *Rs. molischianum* are of the π–π stacking-interaction type. The strengths of π–π stacking interactions between lycopene and aromatic residues were found to be between −2.28 and −6.99 kcal/mol at the MP2/6-31G*(0.25) level (Wang and Hu, 2002b).

The above results suggest that π–π stacking interactions and CH-π interactions between β-carotenes and their surrounding aromatic groups, mostly chlorophylls, play a structural role of stabilizing the pigment-protein complex PS1. In combination with two previous studies (Wang and Hu, 2002b; Mao et al., 2003), the following common features for the structural stabilization role of carotenoids in the photosynthetic pigment-protein complexes emerge. Carotenoid can interact with chlorophyll to stabilize the complex in three different ways:

1. The conjugated core of carotenoid interacts with the tetrapyrrole planes of chlorophyll via π–π stacking interaction.
2. The nonconjugated hydrocarbon ends of carotenoid points toward the tetrapyrrole planes of chlorophyll to form CH-π interactions.
3. The phytol tail of chlorophyll approaches the conjugated core of carotenoid via CH-π interactions.

Results for the first two types of interactions shown in Table 4 indicate that π–π stacking interactions give rise to a slightly stronger interaction strength than CH-π interactions. Preliminary analysis for the third type of interaction also suggests that CH-π interactions between the phytol tail of chlorophyll and the conjugated core of carotenoid have a significant contribution to stabilization. The MP2/6-31G*(0.25) level calculations (data not shown), for example, give rise to an interaction strength of −3.67 kcal/mol for the CH-π interactions between the phytol tail of the chlorophyll molecule CHL1131 and the conjugated core of BCR4017 (see Fig. 2). Carotenoid can also stabilize the protein complex by interacting with the aromatic residues; the latter can approach either the conjugated core of carotenoid via π–π stacking interactions or the nonconjugated hydrocarbon ends of carotenoid via CH-π interactions. Another potential stabilization force is the van der Waals interaction between carotenoid and all amino acids in the protein. However, the magnitude of the van der Waals interactions is relatively weak. The intermolecular interaction energy between the methionine residue M655 and BCR4017 (see Fig. 2), for example, is found to be −0.24 kcal/mol at the MP2/6-31G*(0.25) level of theory.

It has long been believed that the geometric proximity of carotenoid and chlorophyll is necessary for carotenoid to transfer the excitation energy to chlorophyll (light-harvesting role) and to quench the triplet excited state of chlorophyll (photoprotection role) (de Weerd et al., 2003; Naqvi, 1980; Gillbro et al., 1988; Hu et al., 1997). This work firmly established the molecular basis for the third role of carotenoid-chlorophyll stacking, i.e., the structure-stabilization role. The aforementioned structural stabilization role of carotenoids is consistent with the general observation that cofactor binding is needed for some membrane proteins to reach the fully folded state (Chin et al., 2002). It has been reported that binding of retinal to bacteriorhodopsin is essential to protein folding (Lu and Booth, 2000), and so is binding of chlorophylls to the plant light-harvesting complex II (Reinsberg et al., 2001). According to the two-stage model for membrane protein folding, individually stable transmembrane helices are formed in the first stage; they then associate with each other to form a specific tertiary structure in the second stage (Popot and Engelman, 1990). Since the unfolded state is helical already, the cost of conformational entropy to fold the protein is much less in the second stage. As a consequence, relatively weak force is sufficient to drive the association of helices. It is believed that possible driving forces for helix-helix association in the membrane are van der Waals interactions (via close packing) and interhelical hydrogen bonding, including both the conventional and the nonconventional CαH···O hydrogen bonding (Chin et al., 2002). Precise measurement of the free energy change for association of helices in the lipid bilayer is technically challenging. However, estimates suggest that the free energy cost of separating a helix from a helix bundle is 1–5 kcal/mol

(White et al., 2001). In comparison, the magnitudes of nonbonded intermolecular interaction energies between carotenoid and aromatic groups as shown in Table 4 are substantial. Although our calculations deal only with the enthalpy component of the free energy, it is evident that the protein-cofactor interactions play just as important a role as helix-helix interactions in stabilizing the PS1 complex.

It is worth noting that contribution of the zero point energy (ZPE) to the overall intermolecular interaction energy for complex formation should be accounted for in a rigorous quantum chemical treatment. Vibrational frequencies can be obtained from a normal mode analysis; the latter requires the system to be optimized to an energy minimum. Unfortunately, such a normal mode analysis at the MP2 level is not computationally feasible for even the smallest system studied here, i.e., the β-carotene$\cdots$Phe pair that contains 346 electrons with a total of 833 basis functions (1572 primitive Gaussians) at the MP2/6-31G*(0.25) level. However, rigorous normal mode analysis for smaller model systems at high level of theory indicated that the contribution of ZPE in a weakly bonded complex is relatively small in comparison to the intermolecular interaction strength. Karpfen, for example, calculated the intermolecular interaction energy of diacetylene dimer at various configurations at the MP2 level. For the six intermolecular configurations analyzed (see Table 12 in Karpfen, 1999), MP2 calculation resulted in an averaged intermolecular interaction energy and a ZPE correction of -592.7 cm^{-1} (-1.69 kcal/mol) and 32.7 cm^{-1} (0.09 kcal/mol), respectively. It is conceivable that the relatively small ratio of ZPE to the interaction energy (6%) should hold true in our systems as well, mainly because the soft vibrational modes gained as two monomers dimerize have very low frequencies. In addition, it was found that weak intermolecular interactions in the nonbonded complex do not significantly perturb vibrational modes that pre-existed in the monomers (Karpfen, 1999).

Also listed in Table 4 are intermolecular interaction energies at the Hartree-Fock (HF) level. Without exception, the HF/6-31G*(0.25) treatment resulted in an underestimate of interaction energies for the nonbonded intermolecular interactions. In all cases, the HF treatment incorrectly gives rise to positive intermolecular interaction energies (i.e., the wrong sign). This further underscores the point made earlier about the necessity of including correlation correction when dealing with π–π stacking interactions, which is consistent with observations on many other π–π stacking complexes (Sponer et al., 1996a, 2000; Kim et al., 2000; Tsuzuki et al., 1999).

In addition to the total intermolecular interaction energies, its two major components, the dispersion interaction energy and the electrostatic interaction energy, are estimated for each of the pairwise π–π stacking interactions. Results are listed in Table 5. The upper bound for the dispersion interaction energy of the stacking complex was estimated by the correlation component of the MP2 interaction energy (i.e., the difference between the MP2 energy and the HF energy). The correlation component of the MP2 interaction energy ranges from -3.87 kcal/mol for the BCR4007$\cdots$PsaB–F415 pair to as high as -22.86 kcal/mol for the BCR4007$\cdots$CHL1122 pair. The electrostatic interaction energies are determined by the ORIENT 3.2 program using distributed multipoles extracted from the MP2/6-31G*(0.25) wavefunctions of the interacting complex as mentioned in Methods. For all the pairwise intermolecular interactions treated here, the electrostatic interactions are attractive with the exception of the BCR4004$\cdots$CHL1217 pair; the latter has a slightly positive interaction energy of 0.5 kcal/mol. This slightly repulsive electrostatic interaction for the

TABLE 5 Elements of the pairwise intermolecular interaction energies

Intermolecular pair	ΔE_{MP2}* (kcal/mol)	ΔE_{MP2}–ΔE_{HF}† (kcal/mol)	E_{Elec}‡ (kcal/mol)
BCR4004$\cdots$CHL1217	-3.54	-8.95	0.50
BCR4017$\cdots$CHL1239	-12.52	-20.85	-1.45
BCR4014$\cdots$CHL1229	-5.82	-12.60	-0.61
BCR4014$\cdots$CHL1301	-7.61	-10.14	-2.25
BCR4020$\cdots$CHL1131	-8.50	-14.89	-2.67
BCR4007$\cdots$CHL1122	-16.01	-22.86	-1.72
BCR4004$\cdots$CHL1212	-8.03	-13.69	-2.18
BCR4004$\cdots$CHL1218	-8.13	-16.15	-2.10
BCR4017$\cdots$CHL1206	-7.03	-11.03	-1.61
BCR4003$\cdots$CHL1127	-7.48	-12.51	-1.11
BCR4020$\cdots$CHL1207	-9.46	-13.00	-2.87
BCR4020$\cdots$CHL1502	-11.03	-17.72	-3.00
BCR4004$\cdots$PsaB–F224	-0.45	-4.36	-0.70
BCR4020$\cdots$PsaB–W20	-2.51	-4.92	-2.76
BCR4007$\cdots$PsaB–F415	-1.83	-3.87	-0.34

ΔE_{MP2}: total intermolecular interaction energies calculated at the MP2/6-31G(0.25) level with BSSE correction.

†ΔE_{MP2}–ΔE_{HF}: difference between MP2 and HF energies calculated with the 6-31G*(0.25) basis set with BSSE correction, which corresponds to the correlation component of the intermolecular interaction energy.

‡E_{Elec}: electrostatic interaction energies calculated based on a multipole analysis of the MP2/6-31G*(0.25) wavefunctions using the ORIENT 3.2 program (Stone et al., 1995).

BCR4004···CHL1217 pair is an artifact of an unphysical steric clash between the 3-vinyl group of Chl-a molecule CHL1217 and the C14 atom of the β-carotene molecule BCR4004 (see Fig. 4). The unphysical steric clash originated from the limited resolving power of x-ray crystallographic structure determination technique. As stated earlier, in all of our calculations the coordinates of nonhydrogen atoms were taken directly from the x-ray crystal structure. No attempt was made to optimize the intermolecular configurations for fear of its potential for structural distortion.

CONCLUSIONS

We investigated theoretically the structural stabilization role of carotenoids in formation of the photosynthetic pigment-protein complexes. It was hypothesized that π–π stacking and CH-π interactions are the dominant molecular forces that bind carotenoids in the photosynthetic pigment-protein complexes on the basis of a recent data mining analysis that resulted in the discovery that carotenoids are surrounded either by aromatic residues or by chlorophylls in all known crystal structures of the photosynthetic pigment-protein complexes (Wang and Hu, 2002b). The π–π stacking and CH-π interactions between β-carotenes and their surrounding aromatic groups in Photosystem I (PS1) from the cyanobacterium *S. elongatus* were studied by means of the supermolecular approach at the MP2/6-31G*(0.25) level, based on its 2.5 Å resolution crystal structure. PS1 from *S. elongatus* features a core integral antenna system consisting of 90 chlorophyll molecules and 22 carotenoids. The latter are surrounded by a variety of aromatic groups, mainly chlorophylls and in some cases, aromatic residues. The binding pockets of all 22 β-carotenes were classified into six different groups according to position and orientation of their surrounding chlorophylls. One representative β-carotene from each of the six groups was selected for studying configuration dependence of π–π stacking interactions.

The strengths of the π–π stacking interactions between the conjugated core of β-carotene and the tetrapyrrole planes of chlorophyll are found to be substantial, ranging from -3.54 kcal/mol for the perpendicular-positioned BCR4004···CHL1217 pair to -16.01 kcal/mol for the parallel-oriented BCR4007···CHL1122 pair. A strong dependence of the π–π stacking interaction energies on the intermolecular configurations of the two interacting π-planes is observed. The parallel-positioned β-carotene and chlorophyll-a pair is energetically more stable than the perpendicular-oriented pair. The larger the extent of π–π overlapping, the stronger the interaction strength. The strength of π–π stacking interactions decreases as the distance separating the two interacting partners increases. It was also found that in many cases the β-ring ends of β-carotene point toward the tetrapyrrole planes of chlorophyll, forming CH-π interactions. For the latter interactions, the calculated interaction strengths at the MP2/6-31G*(0.25) level varies from -7.03 to -11.03 kcal/mol, depending on the intermolecular configuration.

The physical nature of the intermolecular interactions between β-carotene and chlorophyll (and aromatic amino-acid side chains) was analyzed. The dispersion energy is found to be the dominant intermolecular attractive force. The electrostatic interactions also have a small contribution of attractive force to the binding of β-carotene in PS1.

The significance of the present work is twofold. At first, for carotenoids to function as photoprotection agents of chlorophylls, they have to be bound structurally to the protein in geometrical proximity to the chlorophylls. Until now little has been known about carotenoid binding in the photosynthetic pigment-protein complexes. The present work, along with two previous studies (Wang and Hu, 2002b; Mao et al., 2003), shows that intermolecular π–π stacking interactions and CH-π interactions between carotenoids and their aromatic surroundings are responsible for binding carotenoids. Secondly, the MP2/6-31G*(0.25) calculations showed that π–π stacking and CH-π interactions between closely packed carotenoids and chlorophylls can produce a strong attractive force, which provides the molecular basis for the experimentally observed structure-stabilization role of carotenoids in formation of photosynthetic pigment-protein complexes. In addition to contributing to the understanding of pigment binding, the molecular insight gained in this work will have a direct impact on protein engineering of all pigment-binding proteins.

We thank two anonymous referees for their helpful comments and suggestions, and acknowledge Ohio Supercomputer Center for a generous allocation of supercomputer time.

This work is supported in part through a grant from the deArce Fund for Medical Research and Development.

REFERENCES

Allen, J. P., T. O. Yeates, H. Komiya, and D. C. Rees. 1987. Structure of the reaction center from *Rhodobacter spheroides* R-26: the protein subunits. *Proc. Natl. Acad. Sci. USA*. 84:6162–6166.

Barber, J. 2003. Photosystem II: the engine of life. *Quart. Rev. Biophys.* 36:71–89.

Boys, S., and F. Bernardi. 1970. The calculation of small molecular interactions by the differences of separate total energies. Some procedures with reduced errors. *Mol. Phys.* 19:553–566.

Buckingham, A. D., P. W. Fowler, and J. M. Hutson. 1988. Theoretical studies of van der Waals molecules and intermolecular forces. *Chem. Rev.* 88:963–988.

Chalasinski, G., and M. Gutowski. 1988. Weak interactions between small systems—models for studying the nature of intermolecular forces and challenging problems for ab initio calculations. *Chem. Rev.* 88:943–962.

Chalasinski, G., and M. M. Szczesniak. 2000. State of the art and challenges of the *ab initio* theory of intermolecular interactions. *Chem. Rev.* 100:4227–4252.

Chin, C. N., G. von Heijne, and J. de Gier. 2002. Membrane proteins: shaping up. *Trends Biochem. Sci.* 27:231–234.

Cogdell, R., and H. Frank. 1987. How carotenoids function in photosynthetic bacteria. *Biochim. Biophys. Acta*. 895:63–79.

de Weerd, F. L., J. T. M. Kennis, J. P. Dekker, and R. van Grondelle. 2003. β-carotene to chlorophyll singlet energy transfer in the Photosystem I core of *Synechococcus elongatus* proceeds via the β-carotene S-2 and S-1 states. *J. Phys. Chem. B*. 107:5995–6002.

Deisenhofer, J., O. Epp, K. Miki, R. Huber, and H. Michel. 1985. Structure of the protein subunits in the photosynthetic reaction center of *Rhodopseudomonas viridis* at 3 Å resolution. *Nature*. 318:618–624.

Del Bene, J., and I. Shavitt. 1997. The quest for reliability in calculated properties of hydrogen-bonded complexes. *In* Molecular Interactions. S. Scheiner, editor. Wiley, Chichester, UK.

Eisenschitz, R., and F. London. 1930. Über das Verhältnis der van der Waalsschen Kräfte zu den Homöopolaren Bindungskräften. *Z. Phy.* 60:491–527.

Elstner, M., P. Hobza, T. Frauenheim, S. Suhai, and E. Kaxiras. 2001. Hydrogen bonding and stacking interactions of nucleic acid base pairs: a density functional theory-based treatment. *J. Chem. Phys.* 114:5149–5155.

Ermler, U., G. Fritzsch, S. K. Buchanan, and H. Michel. 1994. Structure of the photosynthetic reaction center from *Rhodobacter sphaeroides* at 2.65 Å resolution: cofactors and protein-cofactor interactions. *Structure*. 2:925–936.

Fraser, N. J., H. Hashimoto, and C. Richard. 2001. Carotenoids and bacterial photosynthesis: the story so far. *Photosynth. Res.* 70:249–256.

Frisch, M. J., G. W. Trucks, H. B. Schlegel, G. E. Scuseria, M. A. Robb, J. R. Cheeseman, V. G. Zakrzewski, J. A. Montgomery, R. E. Stratmann, J. C. Burant, S. Dapprich, J. M. Millam, A. D. Daniels, K. N. Kudin, M. C. Strain, O. Farkas, J. Tomasi, V. Barone, M. Cossi, R. Cammi, B. Mennucci, C. Pomelli, C. Adamo, S. Clifford, J. Ochterski, G. A. Petersson, P. Y. Ayala, Q. Cui, K. Morokuma, D. K. Malick, A. D. Rabuck, K. Raghavachari, J. B. Foresman, J. Cioslowski, J. V. Ortiz, A. G. Baboul, B. B. Stefanov, G. Liu, A. Liashenko, P. Piskorz, I. Komaromi, R. Gomperts, R. L. Martin, D. J. Fox, T. Keith, M. A. Al-Laham, C. Y. Peng, A. Nanayakkara, C. Gonzalez, M. Challacombe, P. M. W. Gill, B. G. Johnson, W. Chen, M. W. Wong, J. L. Andres, M. Head-Gordon, E. S. Replogle, and J. A. Pople. 1998. GAUSSIAN 98, Rev. A.9. Gaussian Inc., Pittsburgh, PA.

Gillbro, T., R. J. Cogdell, and V. Sundström. 1988. Energy transfer from carotenoid to bacteriochlorophyll a in the B800–820 antenna complexes from *Rhodopseudomonas acidophila* strain 7050. *FEBS Lett.* 235:169–172.

Golbeck, J. H. 1992. Structure and function of Photosystem I. *Annu. Rev. Plant Physiol. Plant Mol. Biol.* 43:293–324.

Hobza, P., and J. Sponer. 1996. MP2 and CCSD(T) calculations on H-bonded and stacked formamide···formamide and formamidine···formamidine dimers. *Theochem. J. Mol. Struct.* 388:115–120.

Hobza, P., and J. Sponer. 2002. Toward true DNA base-stacking energies: MP2, CCSD(T), and complete basis set calculations. *J. Am. Chem. Soc.* 124:11802–11808.

Hobza, P., and R. Zahradnik. 1988. Intermolecular interactions between medium-sized systems—nonempirical and empirical calculations of interaction energies—successes and failures. *Chem. Rev.* 88:871–897.

Hobza, P., H. L. Selzle, and E. W. Schlag. 1994. Potential-energy surface of the benzene dimer—ab initio theoretical study. *J. Am. Chem. Soc.* 116:3500–3506.

Hobza, P., J. Sponer, and M. Polasek. 1995. H-bonded and stacked DNA basepairs: cytosine dimer. An ab initio second order Møller-Plesset study. *J. Am. Chem. Soc.* 117:792–798.

Hobza, P., H. L. Selzle, and E. W. Schlag. 1996. Potential energy surface for the benzene dimer. Results of ab initio CCSD(T) calculations show two nearly isoenergetic structures: T-shaped and parallel-displaced. *J. Phys. Chem.* 100:18790–18794.

Hobza, P., J. Sponer, and J. Leszczynski. 1997. Electron-correlated calculations of electric properties of nucleic acid bases—comment. *J. Phys. Chem. B*. 101:8038–8039.

Hofmann, E., P. Wrench, F. Sharples, R. Hiller, W. Welte, and K. Diederichs. 1996. Structural basis of light harvesting by carotenoids: peridinin-chlorophyll-protein from *Amphidinium carterae*. *Science*. 272:1788–1791.

Hsu, C. P., S. Hirata, and M. Head-Gordon. 2001. Excitation energies from time-dependent density functional theory for linear polyene oligomers: butadiene to decapentaene. *J. Phys. Chem. A*. 105:451–458.

Hu, X., T. Ritz, A. Damjanovic, F. Autenrieth, and K. Schulten. 2002. Photosynthetic apparatus of purple bacteria. *Quart. Rev. Biophys.* 35: 1–62.

Hu, X., T. Ritz, A. Damjanović, and K. Schulten. 1997. Pigment organization and transfer of electronic excitation in the purple bacteria. *J. Phys. Chem. B*. 101:3854–3871.

Humphrey, W. F., A. Dalke, and K. Schulten. 1996. VMD—visual molecular dynamics. *J. Mol. Graph.* 14:33–38.

IUPAC-IUB Joint Commission on Biochemical Nomenclature (JCBN). 1986. Nomenclature of tetrapyrroles, recommendations. *Eur. J. Biochem.* 178:277–328.

Jaffe, R. L., and G. D. Smith. 1996. A quantum chemistry study of benzene dimer. *J. Chem. Phys.* 105:2780–2788.

Jordan, P., P. Fromme, H. T. Witt, O. Klukas, W. Saenger, and N. Krauss. 2001. Three-dimensional structure of cyanobacterial Photosystem I at 2.5 Ångstrom resolution. *Nature*. 411:909–917.

Karlstrom, G., P. Linse, A. Wallqvist, and B. Jonsson. 1983. Intermolecular potentials for the H_2O–C_6H_6 and the C_6H_6–C_6H_6 systems calculated in an *ab initio* SCF CI approximation. *J. Am. Chem. Soc.* 105:3777–3782.

Karpfen, A. 1999. The dimer of acetylene and the dimer of diacetylene: a floppy and a very floppy molecule. *J. Phys. Chem. A*. 103:11431–11441.

Kim, K. S., P. Tarakeshwar, and J. Y. Lee. 2000. Molecular clusters of π-systems: theoretical studies of structures, spectra, and origin of interaction energies. *Chem. Rev.* 100:4145–4185.

Koepke, J., X. Hu, C. Münke, K. Schulten, and H. Michel. 1996. The crystal structure of the light-harvesting complex II (B800–850) from *Rhodospirillum molischianum*. *Structure*. 4:581–597.

Kratochvil, M., J. Sponer, and P. Hobza. 2000. Global minimum of the adenine···thymine base pair corresponds neither to Watson-Crick nor to Hoogsteen structures. Molecular dynamic/quenching/AMBER and ab initio beyond Hartree-Fock studies. *J. Am. Chem. Soc.* 122:3495–3499.

Lang, H. P., and C. N. Hunter. 1994. The relationship between carotenoid biosynthesis and the assembly of the light-harvesting LH2 complex in *Rhodobacter sphaeroides*. *Biochem. J.* 298:197–205.

Lokstein, H., L. Tian, J. E. W. Polle, and D. DellaPenna. 2002. Xanthophyll biosynthetic mutants of *Arabidopsis thaliana*: altered nonphotochemical quenching of chlorophyll fluorescence is due to changes in Photosystem II antenna size and stability. *Biochim. Biophys. Acta Bioenerg.* 1553:309–319.

Lu, H., and P. J. Booth. 2000. The final stages of folding of the membrane protein bacteriorhodopsin occur by kinetically indistinguishable parallel folding paths that are mediated by pH. *J. Mol. Biol.* 299:233–243.

Mao, L., Y. Wang, and X. Hu. 2003. π–π stacking interactions in the peridinin-chlorophyll-protein of *Amphidinium carterae*. *J. Phys. Chem. B*. 107:3963–3971.

McDermott, G., S. Prince, A. Freer, A. Hawthornthwaite-Lawless, M. Papiz, R. Cogdell, and N. Isaacs. 1995. Crystal structure of an integral membrane light-harvesting complex from photosynthetic bacteria. *Nature*. 374:517–521.

Moskalenko, A. A., and N. V. Karapetyan. 1996. Structural role of carotenoids in photosynthetic membranes. *Verlag Zeitschr. Naturforsch. C*. 51:763–771.

Naqvi, K. R. 1980. The mechanism of singlet-singlet excitation energy transfer from carotenoids to chlorophyll. *Photochem. Photobiol.* 31:523–524.

Nilsson, R., P. B. Merkel, and D. Kearns. 1972. Unambiguous evidence for the participation of singlet oxygen (1) in photodynamic oxidation of amino acids. *Photochem. Photobiol.* 16:117–124.

Nishio, M., Y. Umezawa, M. Hirota, and Y. Takeuchi. 1995. Tetrahedron report number-378—the CH/π interaction—significance in molecular recognition. *Tetrahedron*. 51:8665–8701.

Popot, J., and D. Engelman. 1990. Membrane protein folding and oligomerization: the two-stage model. *Biochemistry*. 29:4031–4037.

Reinsberg, D., K. Ottmann, P. J. Booth, and H. Paulsen. 2001. Effects of chlorophyll a, chlorophyll b, and xanthophylls on the in vitro assembly kinetics of the major light-harvesting chlorophyll a/b complex, LHCIIb. *J. Mol. Biol*. 308:59–67.

Ritz, T., A. Damjanovic, K. Schulten, J. P. Zhang, and Y. Koyama. 2000. Efficient light harvesting through carotenoids. *Photosynth. Res*. 66: 125–144.

Sponer, J., J. Leszczynski, and P. Hobza. 1996a. Hydrogen bonding and stacking of DNA bases: a review of quantum-chemical *ab initio* studies. *J. Biomol. Struct. Dyn*. 14:117–135.

Sponer, J., J. Leszczynski, and P. Hobza. 1996b. Nature of nucleic acid-base stacking: nonempirical ab initio and empirical potential characterization of 10 stacked base dimers. Comparison of stacked and H-bonded base pairs. *J. Phys. Chem*. 100:5590–5596.

Sponer, J., I. Berger, N. Spackova, J. Leszczynski, and P. Hobza. 2000. Aromatic base stacking in DNA: from ab initio calculations to molecular dynamics simulations. *J. Biomol. Struct. Dyn*. (*Sp. Issue*). S2:383–407.

Stone, A. J. 1985. Distributed polarizabilities. *Mol. Phys*. 56:1065–1082.

Stone, A., A. Dullweber, M. Hodges, and P. Wales. 1995. ORIENT: A Program for Studying Interactions Between Molecules, Ver. 3.2. University of Cambridge, Cambridge, UK.

Tarakeshwar, P., H. S. Choi, and K. S. Kim. 2001. Olefinic vs. aromatic PI-H interaction: a theoretical investigation of the nature of interaction of first-row hydrides with ethene and benzene. *J. Am. Chem. Soc*. 123:3323–3331.

Tsuzuki, S., and H. P. Luthi. 2001. Interaction energies of van der Waals and hydrogen-bonded systems calculated using density functional theory: assessing the PW91 model. *J. Chem. Phys*. 114:3949–3957.

Tsuzuki, S., T. Uchimaru, M. Mikami, and K. Tanabe. 1996. Basis set effects on the calculated bonding energies of neutral benzene dimers: importance of diffuse polarization functions. *Chem. Phys. Lett*. 252:206–210.

Tsuzuki, S., T. Uchimaru, and K. Tanabe. 1998. Intermolecular interaction potentials of methane and ethylene dimers calculated with the Møller-Plesset, coupled cluster and density functional methods. *Chem. Phys. Lett*. 287:202–209.

Tsuzuki, S., T. Uchimaru, K. Matsumura, M. Mikami, and K. Tanabe. 1999. Effects of basis set and electron correlation on the calculated interaction energies of hydrogen-bonding complexes: MP2/cc-pV5Z calculations of H_2O–MeOH, H_2O–Me_2O, H_2O–H_2CO, MeOH-MeOH, and HCOOH-HCOOH complexes. *J. Chem. Phys*. 110:11906–11910.

Tsuzuki, S., T. Uchimaru, K. Matsumura, M. Mikami, and K. Tanabe. 2000. Effects of the higher electron correlation correction on the calculated intermolecular interaction energies of benzene and naphthalene dimers: comparison between MP2 and CCSD(T) calculations. *Chem. Phys. Lett*. 319:547–554.

Tsuzuki, S., K. Honda, T. Uchimaru, M. Mikami, and K. Tanabe. 2002. Origin of attraction and directionality of the π/π interaction: model chemistry calculations of benzene dimer interaction. *J. Am. Chem. Soc*. 124:104–112.

van Mourik, T., and R. J. Gdanitz. 2002. A critical note on density functional theory studies on rare gas dimers. *J. Chem. Phys*. 116:9620–9623.

Wang, Y., and X. Hu. 2002a. Quantum chemical study of π–π stacking interactions of the bacteriochlorophyll dimer in the photosynthetic reaction center of *Rhodobacter sphaeroides*. *J. Chem. Phys*. 117:1–4.

Wang, Y., and X. Hu. 2002b. A quantum chemistry study of binding carotenoids in the bacterial light-harvesting complexes. *J. Am. Chem. Soc*. 124:8445–8451.

White, S. H., A. S. Ladokhin, S. Jayasinghe, and K. Hristova. 2001. How membranes shape protein structure. *J. Biol. Chem*. 276:32395–32398.

Wu, Q., and W. T. Yang. 2002. Empirical correction to density functional theory for van der Waals interactions. *J. Chem. Phys*. 116:515–524.

Wu, X., M. C. Vargas, S. Nayak, V. Lotrich, and G. Scoles. 2001. Towards extending the applicability of density functional theory to weakly bound systems. *J. Chem. Phys*. 115:8748–8757.

Zuber, H., and R. J. Cogdell. 1995. Structure and organization of purple bacterial antenna complexes. *In* Anoxygenic Photosynthetic Bacteria. R. E. Blankenship, M. T. Madigan, and C. E. Bauer, editors. Kluwer Academic Publishers, Dordrecht, The Netherlands. 315–348.

Zurdo, J., C. Fernandez-Cabrera, and J. M. Ramirez. 1993. A structural role of the carotenoid in the light-harvesting II protein of *Rhodobacter capsulatus*. *Biochem. J*. 290:531–537.